Progress In Electromagnetics Research M, Vol. 33, 197–209, 2013

A NOVEL ANTENNA SYSTEM FOR BODY TEMPERATURE CHANGE DETECTION APPROPRIATE FOR MULTI-CHANNEL MICROWAVE RADIOMETRY

Chris D. Nikolopoulos* **and Christos N. Capsalis**

Division of Information Transmission Systems and Material Technology, School of Electrical and Computer Engineering, National Technical University of Athens, 9, Iroon Polytechniou str., Zografou, Athens 15773, Greece

Abstract—A planar inverted F antenna is combined with passive (reactively loaded) elements in order to implement a multi-frequency configuration appropriate for biomedical applications in microwave frequencies. A case study of an electronically Reconfigurable PIFA (R-PIFA) is pursued for the detection of temperature abnormalities in human tissue phantom using microwave radiometry, where the performance of the structure is optimized with respect to input impedance matching in multiple frequencies. The optimization of the array is performed using a Genetic Algorithm (GA) tool as a method of choice. Due to its limited physical size, the proposed R-PIFA can also be used as a portable antenna system for deployment in mobile medical applications.

1. INTRODUCTION

Recently, considerable amount of research and investigation has been focused on properties of malignant tumours related with the increase of temperature in cancerous cells. Temperature and blood flow pattern in cancerous tissues result from two phenomena: heat transfer from the cancer into the surrounding tissues, and vascular reactions. After thorough examination it has been found that temperature in cancer is more than one degree higher than healthy tissue. Microwave radiometry principles can be employed to retrieve sensor information from subcutaneous tissues up to a few centimetres in depth. The development of a non-invasive technique is proposed in this study,

Received 16 September 2013, Accepted 16 October 2013, Scheduled 21 October 2013

* Corresponding author: Chris D. Nikolopoulos (chris.d.nikolopoulos@gmail.com).

where the passive electromagnetic thermal radiation emitted from human body can be monitored using suitable microwave antenna, arranged in an appropriate configuration to cover the concerned area of the body.

Heat can be transferred by three main modes: i) conduction, which requires contact between the objects, ii) convection, where the flow of hot mass transfers thermal energy and iii) radiation. Heat transferred by radiations is of great value in medicine [1]. Natural thermal radiation is the electro-magnetic (EM) radiation from all objects that have a temperature above absolute zero Kelvin. In clinical medicine, microwave radiometry is used to obtain information about internal body temperature patterns by measurement of the natural thermal radiation from the tissues of the human body. The technique is noninvasive, inherently completely safe, and can be used to form an image with low resolution.

Planck's law states that warm bodies emit electromagnetic radiation. In 1900, Max Planck formulated the spectral radiation from a black body. Emission per unit frequency, as a function of frequency (f), is given by:

$$B_f(f) = \frac{2hf^2}{c^2} \frac{1}{e^{\frac{hf}{kT}} - 1} \tag{1}$$

where c is the speed of light, h the Planck's constant, k the Boltzmann's constant, T the temperature, and B_f the spectral radiance. An illustration of spectral radiance at different temperatures versus frequency is given in Fig. 1. Note that the intensity in the infrared range is many orders of magnitude higher than in the microwave range, i.e., from 1 to 10 GHz [2]. Microwave Thermograph (MT) concept is based on measurement of the electromagnetic field spontaneously emitted by a body in microwave frequency range (in our case from 1 to 3 GHz). The intensity of radiation is proportional to body's temperature. Microwaves allow penetration of a few cm enabling internal human tissue temperature measurement [3].

The most important characteristic of the radiometer system is sensitivity defined as the minimum signal threshold that can be detected. The radiometer sensitivity can be described as the standard deviation of the output power. The stochastic input signal to the radiometer is modeled as having zero mean with a variance related to the temperature. If the input noise signal of bandwidth B is integrated over a time τ, the variance is reduced by a factor of $B\tau$. The variance can thus be described by:

$$\sigma^2 \cong \frac{P^2}{B\tau}$$

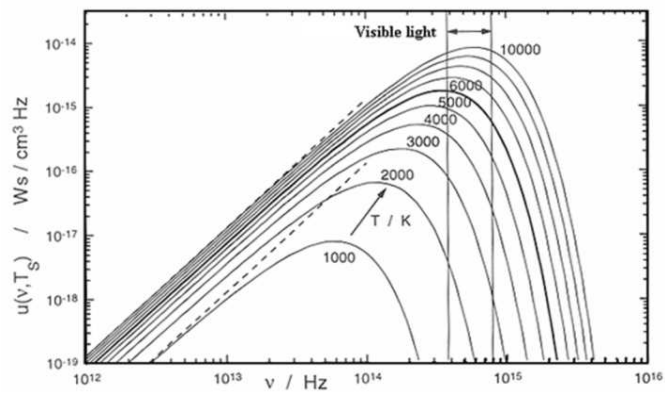

Figure 1. Intensity radiation distribution in respect to frequency and temperature.

The standard deviation or sensitivity of the output is then

$$\Delta T_{\min} = \frac{T_A + T_B}{\sqrt{B\tau}}$$

where τ is the integration time in the lowpass filter of the radiometer. Since the bandwidth (B) cannot be altered because we need a multi-channel characteristics (narrowband channel), it is mandatory to have large time of integration in the RF front end part of the radiometer. There is no significant loss in the output power since the return loss in the antenna part is in minimum (VSWR value close to 1).

From the above, the requirements of this microwave antenna are summarized in the narrowband operation, which will allow the radiometer to distinguish between separate signals coming from different organs and multiple frequency tuning, which will allow the radiometer sensing in several frequencies, resulting in various tissues sensing or detection depths.

The first approach comprises a compact (patch) wideband antenna able to receive microwave signals in the frequency region of few GHz (1 to 3 GHz). The antenna interfaces with a single channel microwave self-balancing modulation radiometer are able to tune in more than one frequency [4–6]. Different wavelengths of the tunable frequency shall penetrate into different depths inside the human tissue, hence providing a series of temperature measurements in succeeding depths [7, 8]. In that way, the main requirement in the design of the antenna is to cover the frequency range mentioned above. So if we assume a central frequency of 2 GHz, the bandwidth of the proposed antenna should be 2 GHz.

The shift in the resonant frequency in these planar antennas is performed by controlling the reactance loaded to a number of passive elements, while there is only one RF output [9–11]. All elements are in short distances from one another, and the consequent strong coupling among them is used in order to control the current flowing into the passive elements. By electrically controlling the loading reactance of the passive elements, changing their electrical size, the central frequency can be configured.

From the authors' knowledge, although the technique using varactor diodes was utilized in the past as a method to get more resonant frequencies in one simple volume [12], the bandwidth achieved has never reached more than 70%. In this paper, a structure is proposed (using a previous work of the author [13]), adding a parasitic element and 3 varactor diodes (reactance loaded), one in the active element and two in the parasitic element, which make the needed percentage (bandwidth) feasible. In that way, the proposed R-PIFA can resonate in any frequency from 1 to 3 GHz and not in a distinctive range as previous work [13], only by controlling the values of the reactance loaded. So we change the entire design and architecture of the previous work (which has a bandwidth of 260 MHz) and develops a new concept (narrowband antenna of 30–40 MHz, but a reconfigurable resonant frequency from 1 to 3 GHz).

2. ARCHITECTURE OF THE 2 ELEMENTS ANTENNA ARRAY

The structure under consideration is depicted in Fig. 2. The active element consists of a top plate connected with the ground plane through a shorting strip and a feed wire. The parasitic element is of the same geometry and orientation, though its wire is not attached to a feed source. By altering the dimensions of the top plates, the height above the ground plane, the size of the ground plane and the distance between the active and parasitic elements, the structure with the best impedance matching at the frequency of operation and adequate bandwidth will be derived.

The structure is generated with the use of SNEC simulation software package, and its performance is optimized by utilizing the Genetic Algorithms (GA) approach. SNEC is a hybrid MoM-UTD (Unified Theory of Diffraction) antenna and electromagnetic simulation program. The MoM primitives available in the code are wire segments, whereas the UTD primitives supported are dielectrically coated plates and elliptical cylinders [14, 15]. The MoM is a numerical electromagnetic technique used to compute the radiation pattern and

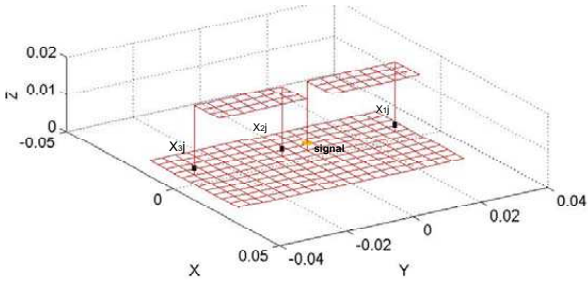

Figure 2. Implementation and analysis of the R-PIFA using wire segments and the SNEC platform.

input impedance of wire-structured antennas [16]. For this reason, the ground plane, top plates, and shorting strips of the R-PIFA were modeled as wire grid plates. The user-defined dimensions for each component of this structure are given in terms of the number of wire segments instead of their physical values. Taking into consideration the fact that the segment length is a fraction of the wavelength, λ, at the simulation frequency, the electrical size of the R-PIFA remains constant with the variation of the operating wavelength. This concept ensures compatibility via the handling of this PIFA structure with the SNEC design procedure. In Fig. 2, the SNEC implementation of the PIFA parasitic is depicted. In order to find an optimum R-PIFA structure with perfect impedance matching and adequate operational bandwidth, the method of GAs is applied. GAs are search methods based on the principles and concepts of natural selection and evolution (crossover, mutation) [17]. A GA is capable of facing multi-variable problems, such as the design and synthesis of antennas, where a set of performance conditions (e.g., input impedance) should be satisfied. In the optimization procedure described herein, the GA module incorporated in SNEC was utilized.

The SNEC results were evaluated via the Finite Elements Method using Asoft HFSS 3D simulation software (High Frequency Structure Simulator — which is offering a linear electromagnetic solution to the physical specified structure based on the finite elements analysis). In the design process which depicted in the Fig. 3 we use copper as the assigned material both for the upper plates and ground plane, also in the sorting strips we add varactor-simulated elements (we model the varactor as resistance + capacitance, for that reason a lumped RLC with proper characteristics was utilized to simulate the effects of the varactor diode, taking into account the resonant frequency of 2 GHz). Finally as a full port impedance we use a resistance of 50 Ohms (to be consistent with the one selected in the SNEC implementation).

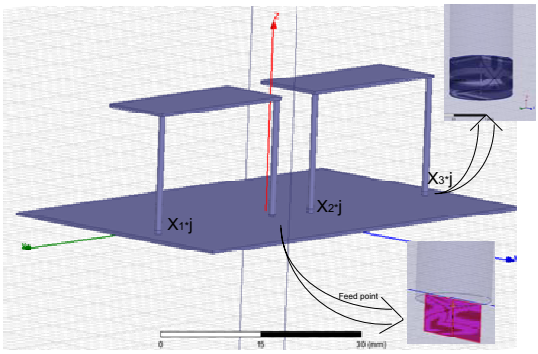

Figure 3. The complete R-PIFA layout using Ansoft HFSS 3D simulation software.

3. OPTIMIZATION PROCEDURE OF THE R-PIFA ANTENNA

3.1. Optimization Parameters and Goals

The goal of the optimization procedure is to operate with maximum gain and minimum reflection coefficient at a band of frequencies (1 to 3 GHz, 50 Ohm input impedance for a 50 Ohm feeding transmission line).

As already mentioned, optimization parameters include the height (h) and width (W) of R-PIFA, and the reactive load values of the passive elements. However, each passive element is independently loaded; therefore all three reactance values of the passive elements participate in the optimization procedure. The optimization parameters are tabulated in Table 1 further below.

3.2. Optimization Range of Reactive Loads

In order to determine the range of the optimization parameters regarding the reactive loads, the matching network of a passive element was simulated using ADS by Agilent [18]. The configuration schematic of the matching network is illustrated in Fig. 4, where the vertical open stub is used in order to emulate an inductor and achieves positive values of the reactive loads range. The variable capacitor C2 is used in order to achieve variable reactive load, while the capacitor C3 is used in order to push the optimization range to negative values and balance the effect of the vertical stub. The left-sided termination is connected to the passive element, while the right-end microstrip is grounded. In order to demonstrate a generic approach, the well-known and popular

Table 1. Input parameters and results of the GA for the R-PIFA at central freq. of 2 GHz ($\lambda_o = 14.99$ cm) and variation of the load reactance of the parasitic elements in a range of frequencies.

Parameter	Variation	Step	GA Results			Physical Dimensions	
Length of the upper plate of each element of the antenna (upLen)	$0.025\lambda_o$–$0.25\lambda_o$	$0.025\lambda_o$	$0.075\lambda_o$			1.124 cm	
Width of the upper plate of each element of the antenna (upWid)	$0.025\lambda_o$–$0.25\lambda_o$	$0.025\lambda_o$	$0.175\lambda_o$			2,623 cm	
Length of ground plane	$0.025\lambda_o$–λ_o	$0.025\lambda_o$	$0.275\lambda_o$			4.122 cm	
Width of ground plane	$0.05\lambda_o$–λ_o	$0.025\lambda_o$	$0.45\lambda_o$			6,746 cm	
Height of wires/shorting strips	$0.025\lambda_o$–$0.25\lambda_o$	$0.025\lambda_o$	$0.125\lambda_o$			1,874 cm	
			1 GHz	1.2 GHz	2 GHz	2.6 GHz	2.8 GHz
Load reactance of the 1st parasitic element (X_1)	$-353j : 111j\ \Omega$	$10j\ \Omega$	$-210j\ \Omega$	$110j\ \Omega$	$-100j\ \Omega$	$-180j\ \Omega$	$-300j\ \Omega$
Load reactance of the 2nd parasitic element (X_2)	$-353j : 111j\ \Omega$	$10j\ \Omega$	$-250j\ \Omega$	$-160j\ \Omega$	$-100j\ \Omega$	$110j\ \Omega$	$110j\ \Omega$
Load reactance of the 3rd parasitic element (X_3)	$-353j : 111j\ \Omega$	$10j\ \Omega$	$-70j\ \Omega$	$-260j\ \Omega$	$0j\ \Omega$	$-240j\ \Omega$	$-300j\ \Omega$

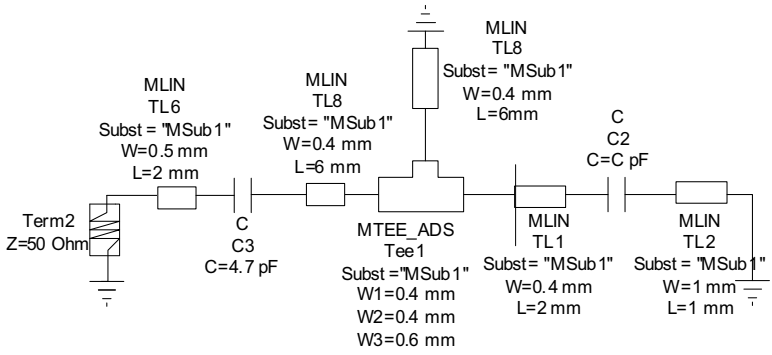

Figure 4. Schematic of a passive element's matching network.

FR4 substrate is used for simulation, with a thickness of 1.6 mm and $\varepsilon_r = 4.6$.

A very large number of commercially available voltage-controlled variable capacitors (varactor diodes) were evaluated, and finally the JDV2S71E diode by Toshiba was selected with frequency range from 0.1–3 GHz. The JDV2S71E diode is an SMD silicon epitaxial diode, with a variable capacitance controlled by in-line DC voltage. Its capacitance values range from 0.64 pF (maximum low capacitance) to 6 pF (minimum high capacitance) for a control voltage ranging from

25 V to 1 V respectively. The simulation results for the schematic of Fig. 4 (from the ADS simulation) when using the JDV2S71E diode are depicted in Fig. 5. The achieved passive element's reactive load ranges from $-353j$ Ohm to $111j$ Ohm [18]. These values are used by the GA in order to generate realistic values for the optimization of the R-PIFA's matching networks.

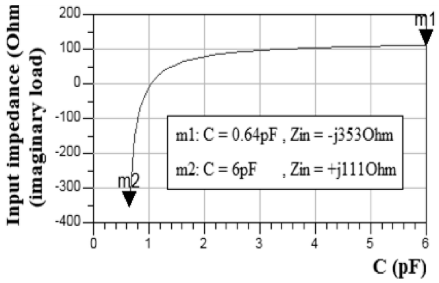

Figure 5. Simulation results for the R-PIFA passive elements' reactive loads.

3.2.1. Objective Function of the GA

The objective function (Of) deployed to obtain desired input impedance level is expressed as:

$$Of = (\mathrm{VSWR_{DES}}/\mathrm{VSWR})^2 \tag{2}$$

where $\mathrm{VSWR_{DES}}$, VSWR are the desired and computed values, respectively [12]. The constraint of $\mathrm{VSWR_{DES}}$ was set equal to 1. The simulation frequency of the first GA was set to be 2000 MHz. The total population consists of 250 generations with 60 chromosomes per generation. The selection method was population decimation, while adjacent fitness pairing was the mating scheme. The crossover point was chosen randomly and each chromosome was divided at a gene level. The mutation probability was equal to 0.15 [14, 15]. As previously stated, Table 1 describes the variation of the parameters that took part in the GA optimization procedure. The proposed PIFA dimensions are expressed in terms of the number of segments. Each segment length was selected to be equal to segment length $= 0.025 * \lambda$. The results of the optimization implementation are exhibited in Table 1. The desired impedance bandwidth is determined by the band of frequencies where the value of the reflection coefficient at the feed point is less than -10 dB, corresponding to a VSWR with a value of no more than 2, when a characteristic impedance of 50 Ω is considered.

As previously mentioned, the scope of the paper is to design a R-PIFA antenna capable to operate in a band of frequencies appropriate for microwave radiometry. Therefore and although the first optimization of the proposed antenna ran for the central resonant frequency of 2 GHz, a lot of GA took place afterwards with the same demands in order to calculate only the values of the reactive loads of the parasitic elements (X_1, X_2, X_3) separately for a band of other frequencies (from 1 GHz to 2.8 GHz) while keeping all the other parameters constant. In that way, we change the resonant frequency by only controlling the values of the reactive loads of the parasitic elements while keeping the geometry and the physical size of the antenna constant. The result of these GA's is also exhibited in Table 1.

4. NUMERICAL RESULTS

Two sets of Genetic Algorithms optimization routines ran, one to optimize the structure (size, VSWR, radiation Pattern) at the central frequency of 2 GHz, and the other set of four different GA's, each one for every frequency depicted in the Fig. 6 with all the parameters constant (taken from the first GA) except for the 3 values of the load reactance of the parasitic elements. The result of the second set of GA's is also depicted in Table 1.

Table 1 describes the variation of the parameters in the GA optimization procedure at the central frequency of 2 GHz, and the respective radiation patterns are depicted in Fig. 7. The proposed array dimensions are expressed in terms of the number of wavelengths and in cm. Each segment length was selected to be equal to 0.025λ. The results of the optimization implementation are exhibited also in Table 1. In Fig. 6, the variation of simulated VSWR in the frequency

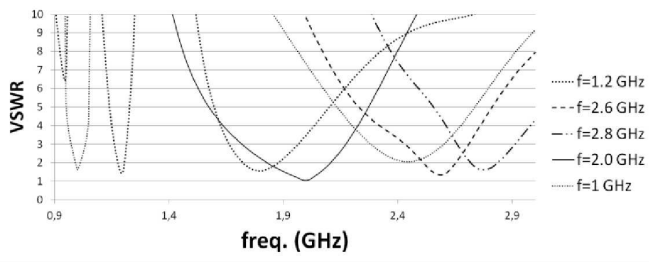

Figure 6. The **SWR** parameter of the optimized array in the frequency band of 1–3 GHz.

range of 1 to 3 GHz is plotted (selected frequencies = 1, 1.2, 2, 2.6, 2.8 GHz).

As shown in Fig. 6, the optimized antenna can exhibit impedance matching (VSWR $\leq$ 2) at any frequency between the range of 1 to 3 GHz (according to the values of the load reactance of the parasitic elements). These values are exhibited in Table 2 for the correspondent frequencies of 1, 1.2, 2, 2.6 and 2.8 GHz. Also, in Figs. 7 and 8, it is shown that the simulated structure demonstrates a main beam towards 90° (elevation), with a 3 dB-beamwidth of 100°, a gain of 2.1 dB, and in the azimuth, the radiation pattern is almost omnidirectional, as confirmed with the HFSS in Fig. 9. It should be noted that these values are maintained through the entire range of 2 GHz operating bandwidth

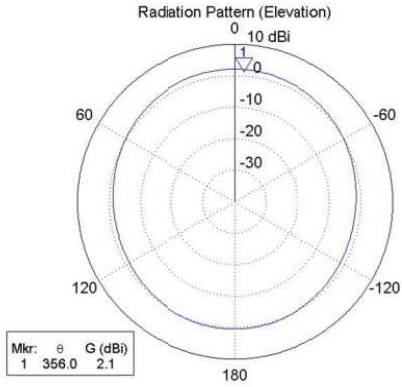

Figure 7. Radiation pattern of the optimized R-PIFA at 2 GHz in the xz plane (elevation) from the SNEC.

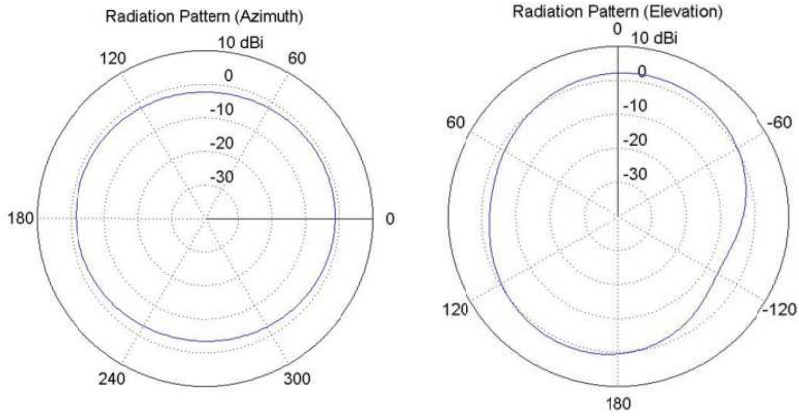

Figure 8. Radiation pattern of the optimized R-PIFA at 2 GHz in the yz plane (elevation), and xy plane (azimuth) from the SNEC.

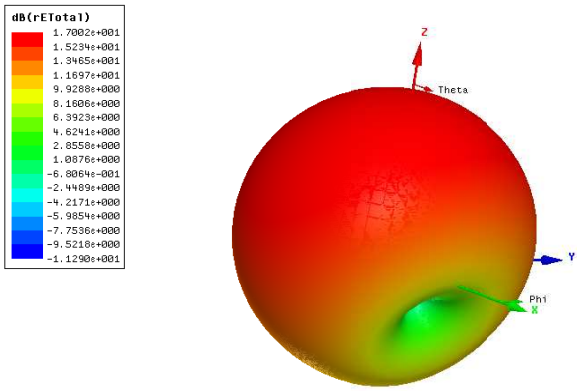

Figure 9. A 3D Radiation pattern of the optimized R-PIFA at 2 GHz using HFSS.

Table 2. Variation of VSWR value with the frequency.

Frequency (GHz)	VSWR
1	1,631
1.2	1,590
2	1,027
2.6	1,366
2.8	1,696

of the proposed structure, thus making the achieved beamwidth and gain quite satisfactory.

5. CONCLUSION

A low-profile Reconfigurable-Pifa is presented in this paper to add new perspectives in the front end (antenna part) of a microwave radiometer offering wider frequency range compared to simple antennas. The operational bandwidth performance was optimized using the technique of the genetic algorithms and the tuning of the resonant frequency achieved by controlling the values of the varacror diodes while the central aim in design was to receive microwave signals in the frequency region of few GHz (1 to 3 GHz). The dynamic tuning range for the band of frequencies we referred is 67.0%. The in-band maximum gain is around 2–2.2 dB throughout the microwave radiometer spectrum. In this paper, the characteristics of a two-element R-PIFA array were studied and analyzed while a bandwidth of 2 GHz are archived for use as the antenna part of a multi-frequency microwave radiometer.

REFERENCES

1. Diakides, N. A. and J. D. Bronzino, *Medical Infrared Imaging*, CRC Press, Taylor & Francis Group, 2008.
2. Leroy, Y., A. Mamouni, J. V. D. Velde, B. Bocquet, and B. Dujardin, "Microwave radiometry for non-invasive thermometry," *Automedica*, Vol. 8, 181–202, 1987.
3. El-Sharkawy, A. M., P. P. Sotiriadis, P. A. Bottomley, and E. Atalar, "A new RF radiometer for absolute noninvasive temperature sensing in biomedical applications," *IEEE International Symposium on Circuits and Systems, ISCAS 2007*, 329–332, 2007.
4. Curto, S., P. McEvoy, X. L. Bao, and M. J. Ammann, "Compact patch antenna for electromagnetic interaction with human tissue at 434 MHz," *IEEE Transactions on Antennas and Propagation*, Vol. 57, No. 9, Sep. 2009.
5. Ohira, T. and K. Gyoda, "Electronically steerable passive array radiator antennas for low-cost analog adaptive beamforming," *Proceedings of the 2000 IEEE International Conference on Phased Array Systems and Technology*, 101–104, May 2000.
6. Bialkowski, M. E., Y. F. Wang, and A. Abbosh, "UWB microwave monopulse radar system for breast cancer detection," *4th International Conference on Signal Processing and Communication Systems (ICSPCS)*, 1–4, Dec. 2010.
7. Bardati, F. and S. Iudicello, "Modeling the visibility of breast malignancy by a microwave radiometer," *IEEE Trans. on Biomed. Eng.*, Vol. 55, No. 1, 214–221, 2008.
8. Iudicello, S. and F. Bardati, "Visibility of breast malignancy in compressed breast by microwave radiometry," *IEEE Antennas and Propagation Society International Symposium, AP-S 2008*, 1–4, Jul. 2008.
9. Sun, C., A. Hirata, T. Ohira, and N. C. Karmakar, "Fast beamforming of electronically steerable passive array radiator antennas: Theory and experiment," *IEEE Transactions on Antennas and Propagation*, Vol. 52, No. 7, 1819–1831, Jul. 2004.
10. Yang, K. and T. Ohira, "Realization of space-time adaptive filtering by employing electronically steerable passive array radiator antennas," *IEEE Transactions on Antennas and Propagation*, Vol. 51, No. 7, 1476–1485, Jul. 2003.
11. Plapous, C., J. Cheng, E. Taillefer, A. Hirata, and T. Ohira, "Reactance domain MUSIC algorithm for electronically steerable parasitic array radiator," *IEEE Transactions on Antennas and Propagation*, Vol. 52, No. 12, 3257–3264, Dec. 2004.

12. Liang, J. and H. Y. D. Yang, "Varactor loaded tunable printed PIFA," *Progress In Electromagnetics Research B*, Vol. 15, 113–131, 2009.
13. Panagiotou, S. C., N. K. Kouveliotis, T. D. Dimousios, P. K. Varlamos, S. A. Mtilineos, and C. N. Capsalis, "A PIFA parasitic optimization utilizing the genetic algorithms technique," *2006 First European Conference on Antennas and Propagation*, 1–5, Nov. 2006.
14. "SuperNec v. 2.4 MOM technical reference manual," Available at: http://www.supernec.com/manuals/snmomtrm.htm.
15. Fourie, A. and D. Nitch, "SuperNEC: Antenna and indoor-propagation simulation program," *IEEE Antennas and Propagat. Mag.*, Vol. 42, No. 3, 31–48, Jun. 2000.
16. Goldberg, D. E., *Genetic Algorithms in Search, Optimization, and Machine Learning*, Addison-Wesley Publishing Company, Inc., 1989.
17. Rahmat-Samii, Y. and E. Michielssen, *Electromagnetic Optimization by Genetic Algorithms*, John Wiley & Sons, Inc., 1999.
18. Dimousios, T. D., S. A. Mitilineos, S. C. Panagiotou, and C. N. Capsalis, "Design of a corner-reflector reactively controlled antenna for maximum directivity and multiple beam forming at 2.4 GHz," *IEEE Transactions on Antennas and Propagation*, Vol. 59, No. 4, 1132–1139, 2011.